NURETH14-405

HEAT TRANSFER PROFILES OF A VERTICAL, BARE, 7-ELEMENT BUNDLE COOLED WITH SUPERCRITICAL FREON-12

G.Richards[1], A.S. Shelegov[2], P.L. Kirillov[3], I.L. Pioro[1], G. Harvel[1]
[1]University of Ontario Institute of Technology, Oshawa, Ontario, Canada
[2]Obninsk State Technical University, Obninsk, Russia
[3]Institute of Physics and Power Engineering, Obninsk, Russia

ABSTRACT

Experimental data on SuperCritical-Water (SCW) cooled bundles are very limited. However, SuperCritical Water-cooled nuclear Reactor (SCWRs) designs cannot be optimized without such data. A set of experimental data obtained in Freon-12 (modeling fluid) cooled vertical bare bundle at the Institute of Physics and Power Engineering (IPPE, Obninsk, Russia) was analyzed. The existence of three distinct regimes for forced convention with supercritical fluids was experienced. (1) Normal heat transfer; (2) Deteriorated heat transfer, characterized by higher than expected temperatures; and (3) Enhanced heat transfer, characterized by lower than expected temperatures. This work compares the heat transfer coefficient of the experiments to predictions based upon current correlations for heat transfer in super critical fluids where the 1-D correlations are based upon tube data under supercritical water conditions.

1. Introduction

One of the six Generation-IV reactor options is a SuperCritical Water-cooled nuclear Reactor (SCWR). The main objective of SCWRs is increasing thermal efficiency of SCW Nuclear Power Plants (NNPs). This reactor type is being developed based on concepts of Light Water Reactors (LWRs), direct-cycle Boiling Water Reactors (BWRs) and supercritical fossil-fuel-fired thermal power plants, especially, their supercritical-pressure turbines' technology. SCWRs are similar to LWRs, but operate at a significantly higher pressure and temperature. [2]

As an alternative to using SuperCritical Water (SCW) as a nuclear-reactor coolant, modeling fluids, for example, such as Freon-12, can be tested as a preliminary approach. The critical parameters of Freon-12 are the following: pressure of 4.13 MPa and temperature of 112ºC, which are significantly lower compared to those of SCW (the critical pressure – P_{cr} = 22.064 MPa and the critical temperature – T_{cr} = 373.95ºC). [3] Therefore, Freon-12 testing will be an easier and cheaper alternative in terms of handling lower pressures, temperatures and heat fluxes compared to those of SCW.

2. Literature Survey

2.1 Modeling Fluids

SCWRs will be cooled with a light-water coolant at a pressure about 25 MPa and within a range of temperatures from 280 – 350°C to 550 – 625°C (inlet to outlet temperatures) [1]. However, these operating conditions can be modeled with lower critical pressure and temperature fluids such as Freons as a preliminary approach. Freon-12 was widely used in industry some time ago as a refrigeration and air-conditioning agent. Therefore, its thermophysical properties are well known within a wide range of conditions including supercritical-pressure region.

Operating conditions of SCWR must be scaled into those of the modeling fluid in order to provide proper SCW-equivalent conditions. Therefore, the following parameters are essential for scaling: pressure, temperature, mass flux, and heat flux. Scaling parameters for fluid-to-fluid modeling at supercritical conditions are summarized in Table 1 [1]. In addition, scaling factors for the conversion of data from Freon-12 to water at supercritical conditions can be found in Table 2. Therefore the experiments that will be discussed in section 3 that were performed at approximately 4.65 MPa in Freon-12 would have a water equivalent pressure of approximately 24.9 MPa, which is close to the proposed to operating pressure of the SCW CANDU reactor.

Table 1. Major scaling parameters for fluid-to-fluid modeling at supercritical conditions based on inlet-conditions approach.

Parameter	Equation
Pressure	$\left(p/p_{cr}\right)_{\mathrm{W}} = \left(p/p_{cr}\right)_{\mathrm{F}}$
Bulk-Fluid Temperature	$\left(T/T_{cr}\right)_{\mathrm{W}} = \left(T/T_{cr}\right)_{\mathrm{F}}$
Heat Flux	$\left(q\,D/k_b \cdot T_b\right)_{\mathrm{W}} = \left(q\,D/k_b \cdot T_b\right)_{\mathrm{F}}$
Mass Flux	$\left(G \cdot D/\mu_b\right)_{\mathrm{W}} = \left(G \cdot D/\mu_b\right)_{\mathrm{F}}$
Heat Transfer Coefficient	$\mathrm{Nu_W} = \mathrm{Nu_F}$

Table 2. Scaling factors for Freon-12 to water at supercritical conditions

Parameter	Equation
Pressure	$\frac{p_W}{p_F} = 5.37$
Temperature	$\frac{T_W}{T_F} = 3.3$
Heat Flux	$\frac{q_W}{q_F} = 20$
Temperature difference	$\frac{\Delta T_W}{\Delta T_F} = 15.4\left(\frac{k_W}{k_F}\right)^{0.66}$

2.2 Experimental studies

A number of studies have been conducted for CO_2 and water at supercritical conditions. These experimental studies cover a wide parameter range. Furthermore, these experimental works are restricted to circular tube geometry. In other words, no publications or correlations are available regarding heat transfer in non-circular tubes [4]. It was shown that at low heat fluxes, an enhancement in the Heat Transfer Coefficient (HTC) was observed as the fluid temperature approaches the pseudocritical point. This phenomena is mostly due to the significant increase in the thermophysical properties of the working fluid; especially its specific heat at the pseudocritical point. Several empirical correlations have been derived from the experimental data. For the purpose of this study, 7 correlations were selected and examined. These correlations are listed below, in Table 3.

Table 3 - List of Nusselt Number Correlations Developed at Supercritical Conditions

	Correlation		**Correlation**
Mokry et al. [5]	$\mathrm{Nu_x} = 0.0061\,\mathrm{Re_x^{0.904}}\,\overline{\mathrm{Pr}}_\mathrm{x}^{0.684}\left(\frac{\rho_\mathrm{w}}{\rho_\mathrm{b}}\right)^{0.564}$	**Gorban et al.** (Freon-12) [8]	$\mathrm{Nu_b} = 0.0094\mathrm{Re_b^{0.86}}\mathrm{Pr_b^{-0.15}}$
Bishop et al. [6]	$\mathrm{Nu_x} = 0.0069\,\mathrm{Re_x^{0.9}}\,\overline{\mathrm{Pr}}_\mathrm{x}^{0.66}\left(\frac{\rho_\mathrm{w}}{\rho_\mathrm{b}}\right)^{0.43}$	**Gupta et al.** [9]	$\mathrm{Nu_w} = 0.004\mathrm{Re_w^{0.923}}\overline{\mathrm{Pr}}_\mathrm{b}^{0.773}\left(\frac{\mu_\mathrm{w}}{\mu_\mathrm{b}}\right)^{0.366}\left(\frac{\rho_\mathrm{w}}{\rho_\mathrm{i}}\right)^{0.186}$
Swenson et al. [7]	$\mathrm{Nu_w} = 0.00459\,\mathrm{Re_w^{0.923}}\,\mathrm{Pr_w^{0.613}}\left(\frac{\rho_\mathrm{w}}{\rho_\mathrm{b}}\right)^{0.231}$	**Dyadyakin et al.** [10]	$\mathrm{Nu_w} = 0.0021\,\mathrm{Re_b^{0.8}}\,\overline{\mathrm{Pr}}_\mathrm{b}^{0.7}\left(\frac{\rho_\mathrm{w}}{\rho_\mathrm{b}}\right)^{0.45}\left(\frac{\mu_\mathrm{b}}{\mu_\mathrm{i}}\right)^{0.2}\left(\frac{\rho_\mathrm{b}}{\rho_\mathrm{i}}\right)^{0.1}$
Jackson et al. [11]	$\mathrm{Nu_w} = 0.0183\,\mathrm{Re_b^{0.82}}\,\mathrm{Pr_b^{0.5}}\left(\frac{\rho_\mathrm{w}}{\rho_\mathrm{b}}\right)^{0.3}\left(\frac{\overline{\mathrm{Cp}}_\mathrm{b}}{\mathrm{Cp_b}}\right)^{\mathrm{n}}$		
Where n is:	$n = 4;\ for\ T_b < T_w < T_{pc}\ \&\ 1.2 * T_{pc} < T_b < T_w$ $n = 0.4 + 0.2\left(\frac{T_w}{T_{pc}} - 1\right);\ for\ T_b < T_{pc} < T_w$	$n = 0.4 + 0.2\left(\frac{T_w}{T_{pc}} - 1\right)\left[1 - 5\left(\frac{T_b}{T_{pc}} - 1\right)\right];$ $for\ T_{pc} < T_b < 1.2 * T_{pc}\ \&\ T_b < T_w$	

3. Experimental Setup

The experimental test section (see Figures 1 and 2) consists of a bare bundle with 7 circular elements installed in a hexagonal flow channel located inside a ceramic insert surrounded by a pressure tube. The bundle has 6 + 1 bare-element arrangement with each element being held at the ends to eliminate the use of spacers. Each of the 7 heating elements has a 9.5-mm outer diameter, and spaced one from another with a pitch of 11.29 mm. The total flow area is 374.0 mm^2, wetted perimeter – 318.7 mm, and hydraulic-equivalent diameter – 4.69 mm.

Main test-section components are cylindrical heated elements (10) installed tightly in the vertical hexagonal shell (12) (downward flow). The entire internal setup is contained by a cylindrical 40 × 4 mm pressure tube with welded flanges at the edges that form the upper (inlet) chamber (6) and lower (outlet) chamber (15), with a total heated length of 1000 mm. Four thermocouples installed into the top and bottom chambers were used to measure Freon-12 inlet and outlet temperatures. Basic parameters of the experimental setup are listed in Table 4.

Table 4. Main experimental-setup parameters for Freon-12 heat transfer experiments.

Pressure	Up to 5.0 MPa
Temperature of Freon-12	Up to 120°C (400°C heating elements)
Maximum mass-flow rate	20 + 20 m^3/h
Maximum pump pressure	1.0 + 1.0 MPa
Experimental test-section power	Up to 1 MW
Experimental test-section height	Up to 8 m
Data Acquisition System (DAS)	Up to 256 channels

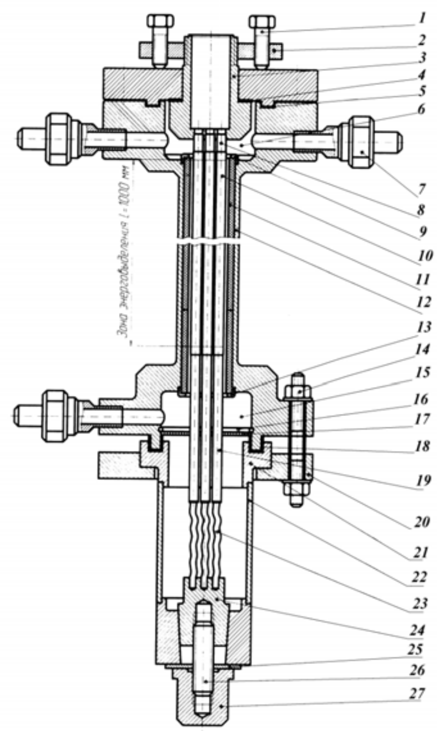

1 – holding-down bolts;
2 – holding-down plate;
3 – upper current terminal;
4 – copper gasket;
5, 18 – insulators;
6 – upper chamber;
7 – union;
8 – copper-tube insert;
9, 13 – clamp rings;
10 – heated elements;
11 – ceramic sleeves;
12 – shell (flow tube);
14 – pin;
15 – lower chamber;
16 – check ring;
17 – Teflon spacer;
19 – copper rods;
20 – lower flange;
21 – adapter;
22 – can;
23 – flexible current leads;
24 – cone;
25 – gasket;
26 – pin;
27 – nut.

Figure 1. Schematic of Experimental test-section used by Shelegov et al. [13]

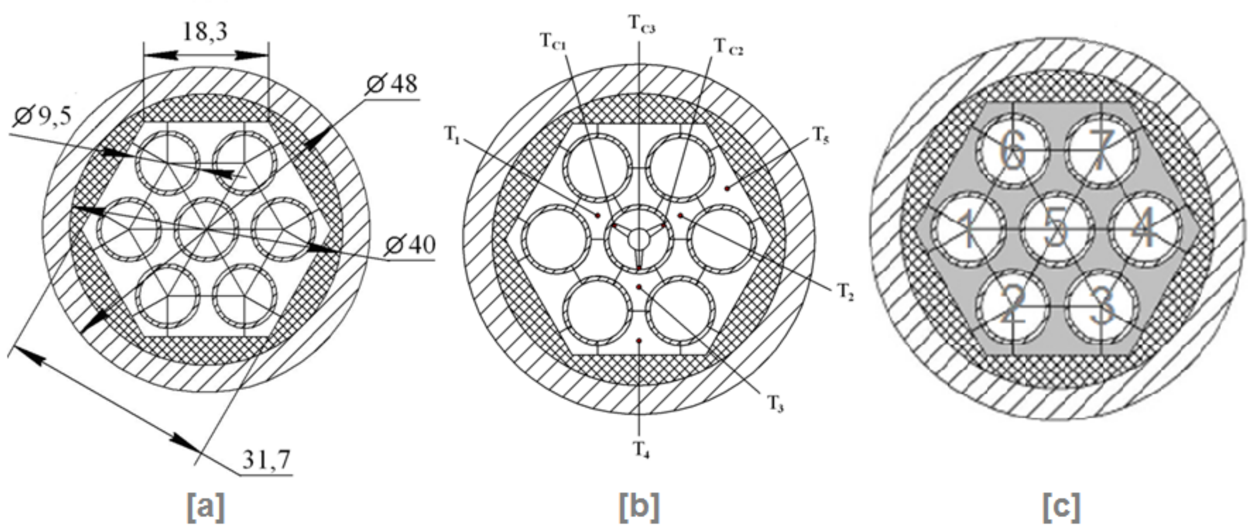

Figure 2. Flow-channel cross sections: (a) with dimensions; (b) with thermocouple layout, and (c) with elements numbering. [12]

Measurements using this setup were only conducted after all necessary operating parameters have been reached and stabilized. These parameters include pressure, temperature, and mass-flow rate. All measurements were collected using DAS to ensure accuracy in control, monitoring, and processing of data. Temperature of the center heated-element sheath was measured using two sliding thermal probes connected to three chromel-copel thermocouples. These three thermocouples were placed at a 120° angle relative to each other as seen in Figure 2. More information on the experimental setup and more specifically the sliding thermal probes can be found Richards et al. 2011. [13]

4. Experimental Results

A total of 20 runs were done using the experimental setup. The dataset can be broken down into three major categories: Below-pseudocritical point, where freon-12 bulk-fluid temperature was below the pseudocritical temperature along the whole heated length of the bundle; Crossing pseudocritical point in which Freon-12 bulk-fluid temperature was below the pseudocritical temperature at the inlet, but reached the pseudocritical temperature at the outlet of the bundle; and finally, above-pseudocritical point, where Freon-12 bulk-fluid temperature was above the pseudocritical temperature along the whole heated length of the bundle. The three major categories can be further divided into smaller groups by the mass flux at which the Freon-12 working fluid is cooling the heated elements. These are: Low Mass Flux: 440 – 520 kg/m^{2}s; Moderate Mass Flux: 990 – 1030 kg/m^{2}s; and High Mass Flux: 1190 – 1320 kg/m^{2}s

Tabular and graphical comparisons of all experiments acquired can be seen in Table 5 and Figure 3, respectively. This data was obtained from Shelegov et al. [12]. Selected cases for each major category can be seen in Figure 4 to Figure 6.

Fluid properties for Freon-12 were taken from NIST RefProp software [3]. In each case bulk fluid temperature was calculated at 1 mm increments along the heated length of the bundle using techniques described in Cengel et al., and Incorpera et al. [14,15]. These techniques can determine the bulk fluid temperature using input parameters from Table 5.

Table 5: Summary of Experimental Dataset obtained from Shelegov et al. [12]

№	P [kW]	G [kg/m^{2}s]	p_{in} [MPa]	p_{out} [MPa]	T_{in} [°C]	T_{out} [°C]
1	2.05	441.3	4.64	4.639	86.13	93.36
2	9.98	447.1	4.629	4.628	89.85	118.75
3	4.05	508.4	4.649	4.645	74.42	91.77
4	11	510.8	4.669	4.664	77.53	114.44
5	14.01	516.9	4.642	4.637	73.78	118.23
6	17	515.6	4.631	4.625	73.39	119.84
7	6.98	517.2	4.635	4.632	111.81	119.86
8	6.99	516.5	4.631	4.629	119.04	125.48
9	9.09	515.6	4.646	4.643	119.26	137.05
10	11.03	1023.6	4.641	4.631	78.64	99.17
Highlighted Rows indicate that temperature profiles for the experiment will be shown below. (Figures 4 – 6)						

№	P [kW]	G [kg/m^{2}s]	p_{in} [MPa]	p_{out} [MPa]	T_{in} [°C]	T_{out} [°C]
11	16.89	1020.2	4.625	4.615	79.95	109.32
12	25	1019.4	4.642	4.63	80.05	117.43
13	9.7	998.2	4.631	4.621	100.2	114.98
14	20.13	1002.6	4.643	4.632	100.41	119.77
15	7.09	1220.2	4.652	4.648	72.86	103.05
16	18.02	1197.4	4.636	4.633	73.26	120.12
17	20.06	1210.0	4.64	4.636	74.08	122.84
18	10	1225.1	4.624	4.622	101.42	121.49
19	13.84	1219.3	4.646	4.644	99.16	125.83
20	16.2	1316.2	4.636	4.632	90.74	121.34
	Below T_{pc}		**Crossing T_{pc}**		**Above T_{pc}**	

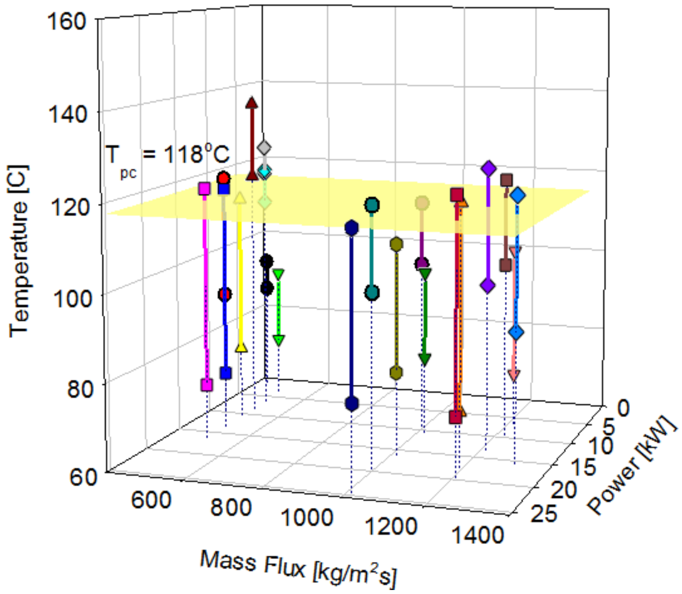

Figure 3: Summary of Experimental Dataset (each line corresponds to a single case performed by Shelegov et al. [13])

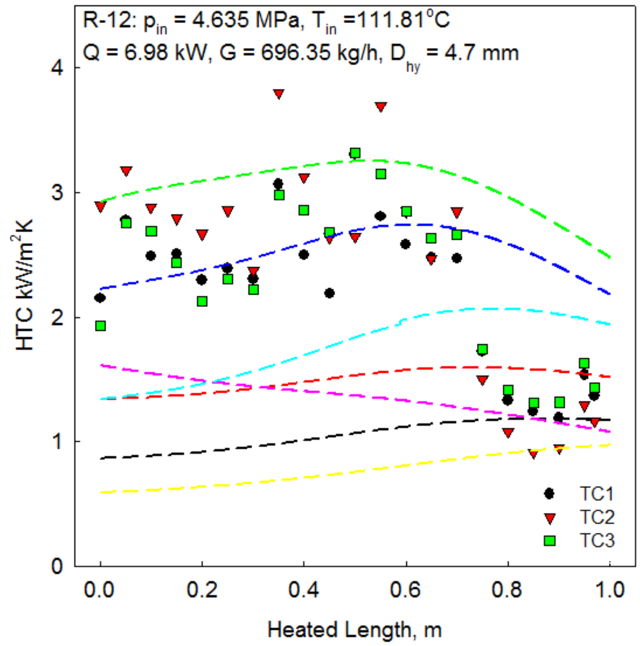

Figure 5: Experiment 7 Heat Transfer Coefficient Profile

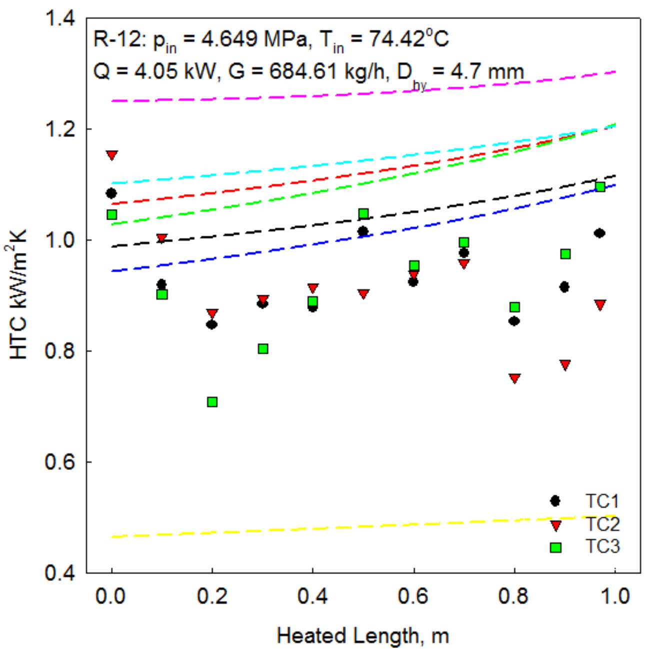

Figure 4: Experiment 3 Heat Transfer Coefficient Profile

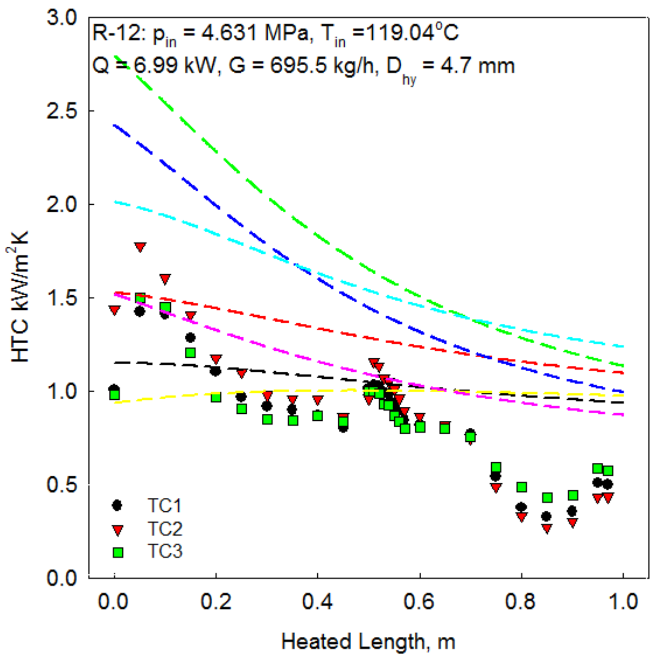

Figure 6: Experiment 8 Heat Transfer Coefficient Profile

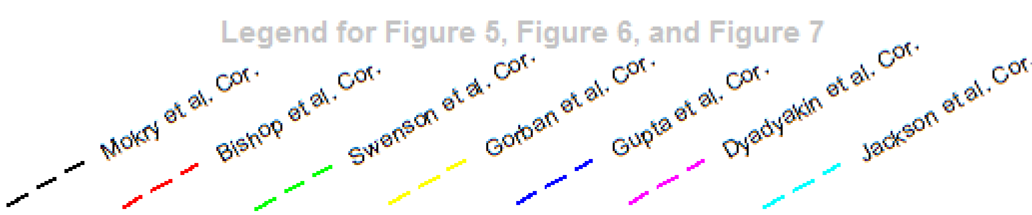

Experiments 1, 3, 4, and 10 demonstrate only the normal heat transfer regime while all other cases demonstrate normal heat transfer with either one or two segments in the deteriorated heat transfer (DHT) regime. In all cases demonstrating DHT, the regime was experienced near the end of the heated section (between 0.8m and 1.0m). In cases experiencing two areas of DHT, the second regime was experienced after approximately 0.2m. Figure 7 to Figure 13 show a comparison of the HTC data with those calculated according to each of the 7 correlations. No single existing correlation was able to predict the experimental HTC near or above the pseudocritical point in all experimental data sets provided by Shelegov et al. [12].

The Mokry et al. and Bishop et al. correlation appear to stratify with no pattern and were not able to predict the experimental data effectively. The majority of the data points could not be predicted within ±50% error. The Swenson et al. correlation consistently over predicts the experimental HTC, however with error greater than ±100% for a number of points. When using the Gorban et al. correlation, experimentally calculated HTC was consistently under predicted with error of greater than ±50%. The remaining correlations (Gupta et al., Dyadyakin et al., and Jackson et al.) could not predict the experimental HTC with ±50% and do not approximate the data with any pattern.

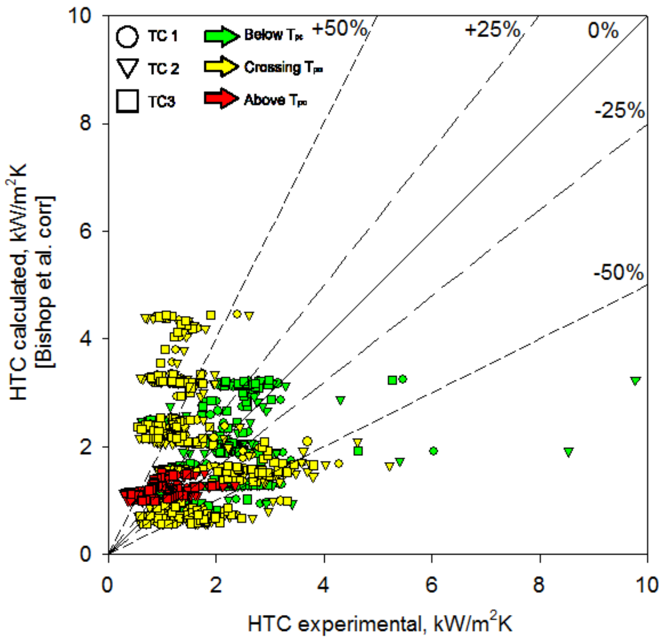

Figure 8: Comparison of Experimental HTC Values with those calculated with the Bishop et al correlation.

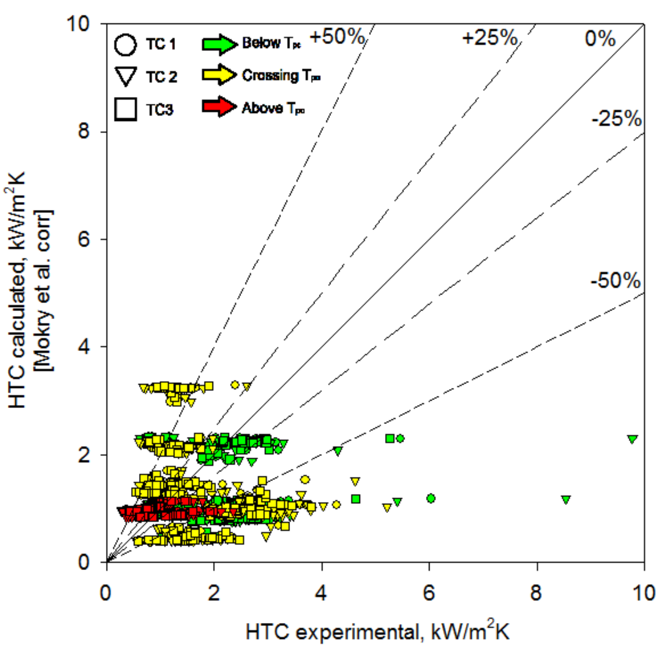

Figure 7: Comparison of Experimental HTC Values with those calculated with the Mokry et al correlation.

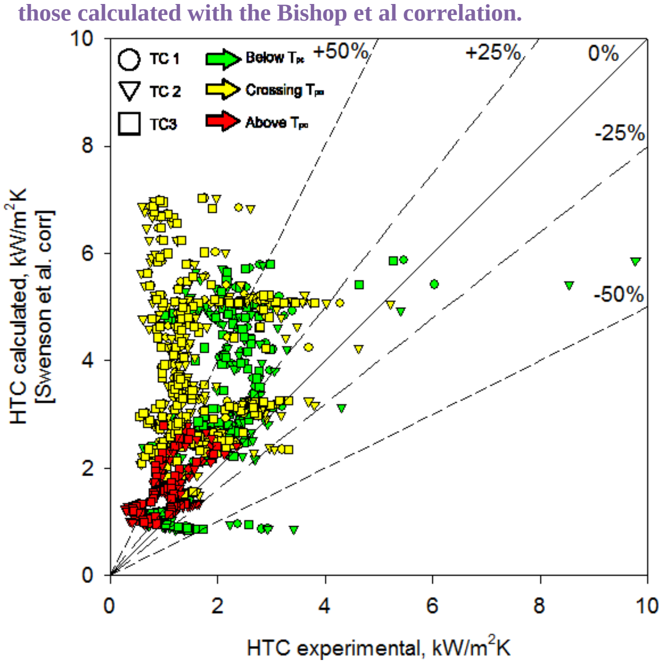

Figure 9: Comparison of Experimental HTC Values with those calculated with the Swenson et al correlation.

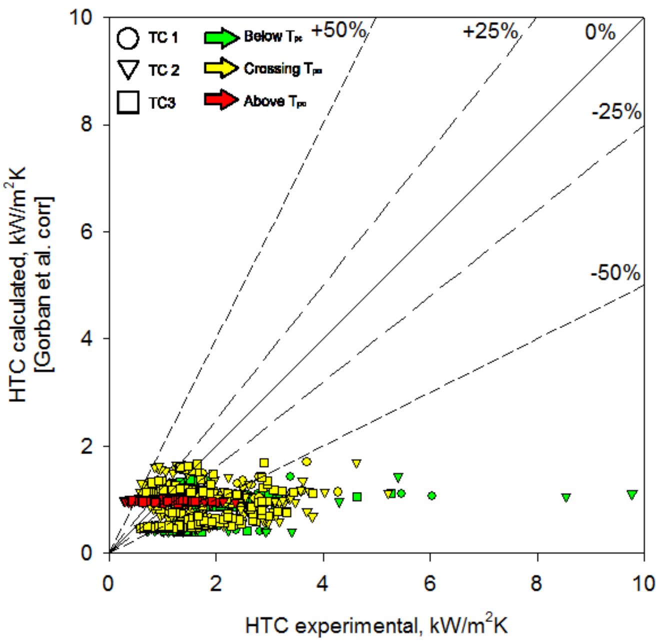

Figure 10: Comparison of Experimental HTC Values with those calculated with the Gorban et al correlation.

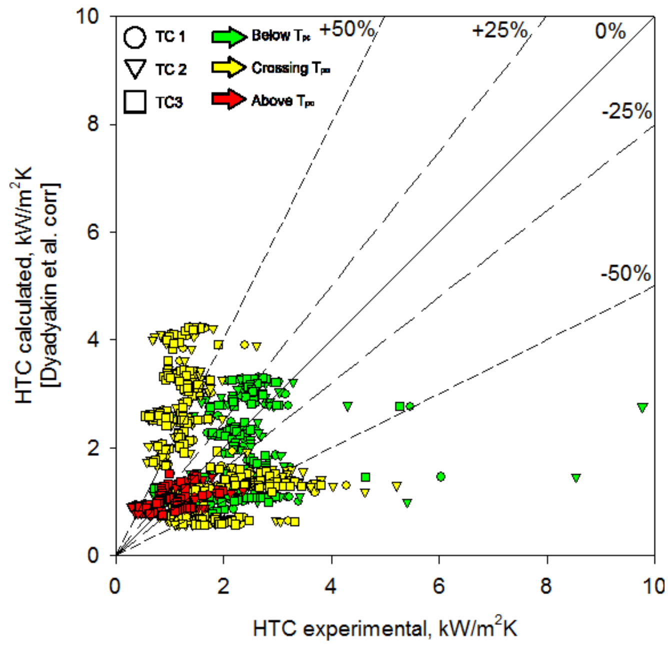

Figure 12: Comparison of Experimental HTC Values with those calculated with the Dyadyakin et al correlation

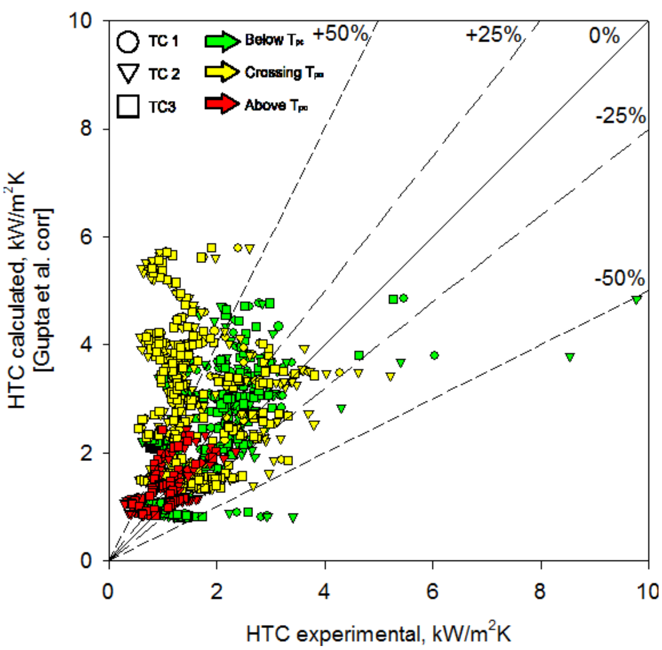

Figure 11: Comparison of Experimental HTC Values with those calculated with the Gupta et al correlation.

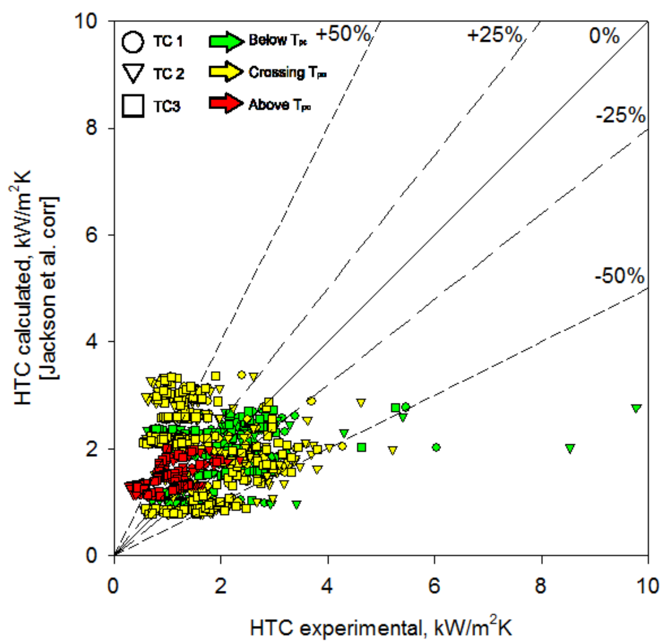

Figure 13: Comparison of Experimental HTC Values with those calculated with the Jackson et al correlation.

5. Concluding Remarks

The experiments have been conducted in a vertical 7-element bundle cooled with upward flow of supercritical Freon-12. The experiments showed that at certain operating conditions the deteriorated heat-transfer regime is possible not only in bare tubes, but also in "bare" bundles. In previous studies conducted with bundles fixed with helical fins, regions of deteriorated heat-transfer have not been encountered when cooled with supercritical fluids.

In general, no single existing Nusselt correlation is able to accurately predict the experimental data for all cases. The correlations were not able to come within ± 50% of the experimental heat transfer coefficient. For specific cases some correlations were able to closely approximate heat transfer coefficient in the normal regime, however deteriorated/improved heat transfer regimes could not be predicted. A new correlation must be made, taking into account the causes of different heat transfer regimes in order to more accurately predict data for bare bundles cooled with supercritical fluids.

Further analysis and must be completed regarding the effect of bundle geometries on the deterioration of heat transfer from the elements to the working fluid as there are many unpredicted changes in heat transfer coefficient along in the heated length of the test section. Also, investigation on the effect of the working fluid (supercritical freon vs. supercritical water) on the level of heat transfer deterioration must be considered in order to accurately model DHT in bundles cooled with supercritical fluids.

6. Nomenclature

$\bar{c}_p$	averaged specific heat; $\left(\frac{H_w - H_b}{T_w - T_b}\right)$, J/kg K
D	diameter, mm
G	mass flux, kg/m^{2}s; $\left(\frac{m}{A_{fl}}\right)$
k	thermal conductivity, W/m K
m	mass-flow rate, kg/s; (ρV)
p	pressure, MPa
P	power, kW
q	heat flux, kW/m^2
Q	heat-transfer rate, kW
T	temperature, K

6.1 Greek Letters

μ	dynamic viscosity, Pa s
ρ	density, kg/m^3

6.2 Non-Dimensional Numbers

Nu	Nusselt number; $\left(\frac{h\,D}{k}\right)$
Pr	Prandtl number; $\left(\frac{\mu\, c_p}{k}\right) = \left(\frac{\upsilon}{\alpha}\right)$
$\overline{\text{Pr}}$	averaged Prandtl number; $\left(\frac{\mu\ \bar{c}_p}{k}\right)$
Re	Reynolds number; $\left(\frac{G\,D}{\mu}\right)$

Symbols with an overline denote average or values (e.g., $\overline{\text{Nu}}$ denotes average (mean) Nusselt number).

6.3 Subscripts or Superscripts

b	bulk
hy	hydraulic
pc	pseudocritical
w	wall/sheath

6.4 Abbreviations and Acronyms

AECL	Atomic Energy of Canada Limited
DHT	Deteriorated Heat Transfer
HTC	Heat Transfer Coefficient
IPPE	Institute of Physics and Power Engineering (Obninsk, Russia)
NIST	National Institute of Standards and Technology
NPP	Nuclear Power Plant

SCR	SuperCritical Reactor	SCWR	SuperCritical Water-cooled Reactor
SCW	SuperCritical Water		

7. Acknowledgments

Financial supports from the NSERC Discovery Grant and NSERC/NRCan/AECL Generation IV Energy Technologies Program (NNAPJ) are gratefully acknowledged.

Special thanks to Jeffery Samuel and Amjad Farah for their valuable discussion.

8. References

[1] Pioro, I.L. and Duffey, R.B., Heat Transfer and Hydraulic Resistance at Supercritical Pressures in Power Engineering Applications, ASME Press, New York, NY, USA, 2007, 334 pages.

[2] GIF – Generation IV International Forum, "A Technology Roadmap for Generation IV Nuclear Energy Systems, Issued by the Generation IV international Forum and the U.S. DOE Nuclear Energy Research Advisory Board, 2002.

[3] National Institute of Standards and Technology, 2007. NIST Reference Fluid Thermodynamic and Transport Properties-REFPROP. NIST Standard Reference Database 23, Ver. 8.0. Boulder, CO, U.S.: Department of Commerce.

[4] Cheng, X., & Schulenberg, T. (2001). *Heat transfer at supercritical pressures-literature review and application to an HPLWR.* Retrieved 9 18, 2009, from http://bibliothek.fzk.de/zb/berichte/FZKA6609.pdf

[5] Mokry, S., Gospodinov, Y., Pioro, I.L., "Supercritical Water Heat-Transfer Correlation for Vertical Bare Tubes", Proceedings of the International Conference on Nuclear Engineering (ICONE-17), Brussels, Belgium, 2009, July 12-16.

[6] Bishop, A.A., Sandberg, R.O., and Tong, L.S., 1964. High Temperature Supercritical Pressure Water Loop: Part IV, Forced Convection Heat Transfer to Water at Near-Critical Temperatures and Super-Critical Pressures, Westinghouse Electric Corporation, Pittsburgh, Pennsylvania.

[7] Swenson, H.S., Carver,J.R., and Kakarala, C.R, 1965. Heat Transfer to Supercritical Water in Smooth-Bore Tubes, J. of Heat Transfer, Trans. ASME Series C, 87 (4), pp. 477-484.

[8] Gorban, L.M., Pomet'ko, R.S., Khryaschev, O.A., 1990. Modeling of water heat transfer with Freon of supercritical pressure, (in Russian). -1766, Institute of Physics and Power Engineering, Obninsk, Russia. 1990

[9] Gupta, S., Mokry, S., Farah, A., King, K., Pioro, I.L., "Developing a new heat-transfer correlation for supercritical-water flow in vertical bare tubes", Proceedings of the International Conference on Nuclear Engineering (ICONE-18), Xi'an, China, 2010, May 17-21.

[10] Dyadyakin, B.V. and Popov, A.S., 1977. Heat transfer and thermal resistance of tight seven-rod bundle, cooled with water flow at supercritical pressures, (In Russian), Transactions of VTI (Труды ВТИ), No. 11, pp. 244–253.

[11] Jackson, J.D., 2002. Consideration of the Heat Transfer Properties of Supercritical Pressure Water in Connection with the Cooling of Advanced Nuclear Reactors, Proc. 13th Pacific Basin Nuclear Conference, Shenzhen City, China, October 21-25.

[12] Shelegov A.S., Leskin S.T., Chusov I.A., Slobodchuk V.I. Experimental Investigation of Heat Transfer in the 7-rod bundle under Supercritical Parameters of Freon-12 / Preprint IATE 001-2010. - Obninsk: IATE NRNI MEPhI, 2010.-42 P.

[13] Richards, G., Shelegov, A.S., Kirillov, P.L., Pioro, I.L., Harvel, G., 2011. Temperature Profiles of a Vertical Bare 7-Element Bundle Cooled with Supercritical Freon-12, Proceedings of the 19th International Conference On Nuclear Engineering (ICONE-19), Chiba, Japan, May 16-19, Paper to be published.

[14] Cengel, Y. and Ghajar, A. “Heat and Mass Transfer”, McGraw Hill, USA, 2006.

[15] Incropera, F. P., Dewitt, D. P., Bergman, T. L., and Lavine, A. S., “Fundamentals of Heat and Mass Transfer”, John Wiley and Sons, USA, 2006.